Optimal Power Flow in DC Networks with Robust Feasibility and Stability Guarantees

Jianzhe Liu, *Member, IEEE*, Bai Cui, *Member, IEEE*, Daniel K. Molzahn, *Senior Member, IEEE*, Chen Chen, *Senior Member, IEEE*, and Xiaonan Lu, *Member, IEEE*

***Abstract*— With high penetrations of renewable generation and variable loads, there is significant uncertainty associated with power flows in DC networks such that stability and operational constraint satisfaction are of concern. Most existing DC network optimal power flow (DN-OPF) formulations assume exact knowledge of loading conditions and do not provide stability guarantees. In contrast, this paper studies a DN-OPF formulation which considers both stability and operational constraint satisfaction under uncertainty. The need to account for a range of uncertainty realizations in this paper's robust optimization formulation results in a challenging semi-infinite program (SIP). The proposed solution algorithm reformulates this SIP into a computationally tractable problem by constructing a tight convex inner approximation of the stability set using sufficient conditions for the existence of a feasible and stable power flow solution. Optimal generator set-points are obtained by optimizing over the proposed convex stability set. The validity and effectiveness of the propose algorithm is demonstrated through various DC networks adapted from IEEE test cases.**

I. Introduction

Recent years have witnessed the growth of DC loads and generators, such as DC fast charging facilities, photovoltaic generation, and various electronic devices in sites like data centers. Interconnecting DC components in a DC network is an efficient operation method due to the reduction of DC-AC conversion stages [1]. DC networks have thus found promising applications in low- and medium-voltage power systems such as community nanogrids and microgrids, shipboard power systems, data centers, etc. [2]. Common features of DC networks include: 1) the loading conditions are usually uncertain and 2) many loads are controlled as constant power loads (CPLs) that have destabilizing negative impedance effects [2].

Similar to other power systems, a DC network should work at a stable operating point that satisfies all operational constraints. The classic method to compute such an operating point is to formulate and solve an optimal power flow (OPF) problem. An OPF problem finds the optimal generation schedule corresponding to the system operating point that maximizes economic welfare while satisfying various physical and operational constraints. OPF problems are usually computationally challenging to solve [3].

Many research efforts have improved the tractability of OPF problems for AC power systems using approximation and relaxation methods [4]. Recent research has also studied OPF problems for DC networks (DN-OPF) [5]–[11]. Note that DN-OPF problems are fundamentally different from so-called "DC-OPF" problems [12]. Whereas DC-OPF problems linearize the nonlinear power flow equations for an AC power system, DN-OPF problems consider the nonlinear power flow equations that accurately model the physics of a DC network. This makes a typical DN-OPF problem a non-convex optimization problem [9].

A variety of methods have been applied to solve DN-OPF problems. In [5], a genetic algorithm is applied to solve the OPF problem for a DC distribution system. In [13], linearization techniques are used to simplify the problem. Other methods [6]–[8] employ second-order cone programming and quadratic convex programming to relax a DN-OPF problem into a convex formulation. This existing work demonstrates the capability to effectively solve various DN-OPF problems.

Despite recent advances, existing DN-OPF work [6]–[8] has limitations in providing stability and feasibility guarantees when significant uncertainties are present. First, previous results primarily focus on deterministic DN-OPF problems where the loading conditions are assumed to be fixed and known *a priori*. Nevertheless, with high penetrations of intermittent generation and variable loads, uncertainty in the net loading conditions is a salient feature of DC networks [14]. Directly applying the OPF decisions computed using a specific scenario to an uncertain system can cause unpredictable deviations of the system operating point from the designated value [15], [16]. This may lead to violations of operational constraints and possibly cause voltage collapse. For example, unexpected DC fast charging events or loss of renewable generation can make the system unable to accomplish the load supporting task, in which case the power flow equations cease to admit a solution [17], [18].

Second, previous results do not consider stability issues of DN-OPF solutions. A DC network has rich dynamics contributed by electrical circuits and control systems [1], [19], which are subject to notable risks of instability associated with the choice of operating point [20]–[24]. Many loads in a DC

J. Liu is with the Energy Systems Division, Argonne National Laboratory, Lemont, IL 60439, USA. Email: jianzhe.liu@anl.gov.

B. Cui is with the Power Systems Engineering Center, National Renewable Energy Laboratory, Golden, CO 80401, USA. Email: bcui@nrel.gov.

D. Molzahn is with the School of Electrical and Computer Engineering, Georgia Institute of Technology, Atlanta, GA 30332, USA. Email: molzahn@gatech.edu.

C. Chen is with the School of Electrical Engineering, Xi'an Jiaotong University, Shaanxi, China. Email: morningchen@xjtu.edu.cn.

X. Lu is with the College of Engineering, Temple University, Philadelphia, PA 19122, USA. Email: xiaonan.lu@temple.edu.

network can be considered as CPLs that are known to have harmful negative impedance effects. If the operating point is not carefully selected, the system can be under-damped or even become unstable [19], [20].

We propose a stability-constrained robust DN-OPF algorithm to address these limitations. Following from DC network operation practices, we focus on a DC network with nonlinear CPLs and controllable voltage sources. We seek to minimize system operational costs by computing setpoints for the sources which rigorously guarantee the following two properties for any loading condition within a specified uncertainty set: 1) robust feasibility (existence of power flow solutions satisfying operational constraints) and 2) robust stability (local exponential stability of the operating point).

To provide such guarantees, we formulate a DN-OPF problem that incorporates uncertainty and stability conditions. Solving this problem is difficult. First, existing stability conditions for DC networks are developed to study given operating points [25]; hence, ensuring stability when operating points are decision variables is challenging. Additionally, to ensure robustness, the power flow equations along with the stability conditions need to jointly hold for all uncertainty realizations. This results in a semi-infinite programming (SIP) problem [26] that is generally computationally intractable [27]. Tractable reformulations or approximations exist for robust optimization problems when special structures of problem formulation and data uncertainty can be exploited [28]; however, there are no standard approaches to deal with the non-convexity associated with the power flow equations.

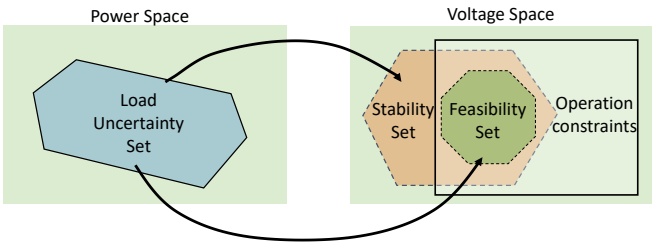

Fig. 1. Illustration of the proposed work.

The proposed algorithm converts the SIP problem into a tractable formulation that resembles a well-studied DN-OPF problem. The main idea of the proposed work is illustrated in Fig. 1, and we summarize the main technical tasks as follows:

(1) We first derive a stability set in the voltage space such that any operating point therein is guaranteed to be stable.
(2) We then develop conditions which guarantee the existence of a power flow solution that is feasible with respect to the operational constraints. We characterize the boundaries of the set of feasible operating points defined by these conditions.
(3) Finally, we formulate and solve a tractable problem reminiscent of a DN-OPF problem to ensure that the entirety of the set of operating points lies in the intersection of the stability set and the operational constraints.

The contributions of the paper are:

- We develop a novel algorithm to reformulate and solve a class of otherwise intractable DN-OPF problems using a synthesis of new DC network stability analysis and power flow feasibility results;
- We provide a new condition on the solvability of DC network power flow equations and new methods to compute a stability set. The solvability condition enables one to find the exact upper and lower bounds for feasible power flow solutions, i.e. the DC bus voltages.
- The proposed work provides insights into DC network operation. For example, the solvability condition theoretically validates typical engineering practices that attempt to ensure acceptable operation despite a range of uncertainty via the use of representative scenarios.

The rest of the paper is organized as follows: First, Section II introduces the system model and the main problem considered in this paper. Next, Section III shows the main results of the paper, i.e., a solution algorithm for a robust DN-OPF problem with feasibility and stability guarantees. Section IV then demonstrates the efficacy of the proposed work using simulation case studies. Finally, Section V concludes the paper and discusses future research directions.

II. System Modeling and Problem Statement

A. Notation

In this paper, we use $\mathbf{1}$ and $\mathbf{0}$ to represent vectors of all 1's and 0's of appropriate sizes, and use $\mathbf{I}$ to represent the identity matrix of appropriate size. Recall that a square matrix A is Hurwitz if all real parts of its eigenvalues are negative. In addition, we use $A_{j,k}$ to denote the element on the j-th row and k-th column of the matrix A. For a vector v, let v_k represent its k-th element. Let the operator $\mathrm{diag}\{v\}$ yield a diagonal matrix with the vector's components being the diagonal entries. The matrix transpose operator is denoted by $(\cdot)^\top$. For a real square matrix A, A^{-1} denotes its inverse, $A \succ 0$ (resp., $A \succeq 0$) means it is symmetric positive definite (resp., semidefinite), and $A \prec 0$ (resp., $A \preceq 0$) means $-A \succ 0$ (resp., $-A \succeq 0$).

B. DC Power Systems

In this paper, we focus on a DC network with n_s generators, n_ℓ loads, and n_t power lines. The total number of these components is $n = n_s + n_t + n_\ell$. Let the index sets of generators, loads, and power lines be $\mathcal{N}_s$, $\mathcal{N}_\ell$, and $\mathcal{E}_t$, respectively. Fig. 2 shows an example DC network consisting of lumped π-equivalent models [24] where generators and loads are interconnected via equivalent RLC circuits [1].

1) Load and Generator Models: Fig. 3 shows a zoomed-in image of one part of the circuit. Suppose the circuit has the k-th generator, p-th power line, and j-th load. Let $i_{to}(t)$ and $i_{td}(t)$ represent the current flowing into and out of the circuit.

Loads are modeled as constant power loads (CPLs) that are connected in parallel with a lumped shunt resistor by Norton's Theorem. It is well known that CPLs are nonlinear loads and that their associated negative impedance effects are major sources of instabilities in DC networks [21], [29]. CPLs are modeled as a nonlinear current source with current injection equal to the power output divided by terminal voltage.

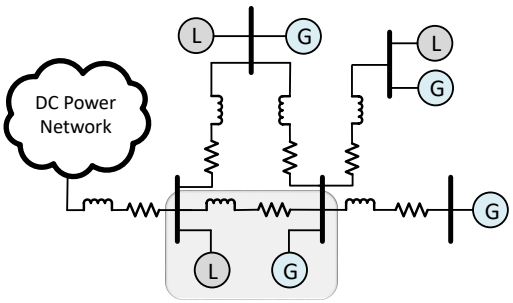

Fig. 2. Example DC power network.

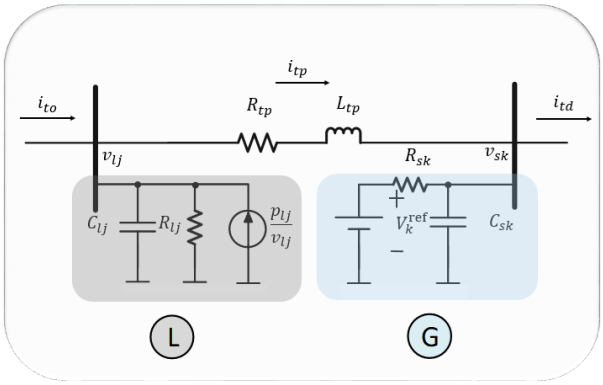

Fig. 3. Zoomed-in image of the dynamic circuit.

For the k-th load, let $p_{\ell k}$ represent its power injection into the network, and let $v_{\ell k}$ represent the terminal voltage. At the nominal condition, $p_{\ell k} = p^*_{\ell k}$, where $p^*_{\ell k}$ is a given constant. Each $p_{\ell k}$ is considered to be a perturbation to $p^*_{\ell k}$ that is unknown and bounded within a given uncertainty interval $[\underline{p}_{\ell k}, \bar{p}_{\ell k}]$. Throughout this paper, we let positive $p_{\ell k}$ represent positive power injection (i.e., power generation) at bus k. In addition, we assume that $\bar{p}_{\ell k} \geq 0$ and $\underline{p}_{\ell k} \leq 0$. Let $\mathcal{P}_\ell$ be the interval uncertainty set for all load, that is, $\mathcal{P}_\ell = \{p_\ell : p_{lk} \in [\underline{p}_{\ell k}, \bar{p}_{\ell k}], k \in \mathcal{N}_\ell\}$. Let $R_{\ell j}$ and $C_{\ell j}$ represent the load resistance and capacitance, respectively.

For the k-th source, let V_k^{ref} be the controllable voltage setpoint, v_{sk} be the external generator voltage, and R_{sk}, C_{sk} represent the source resistance and capacitance, respectively. We impose operational constraints on controllable voltage setpoints such that vector V^{ref}, which includes all voltage setpoints, needs to lie within a given convex constraint set $\mathcal{V}^{\text{ref}}$.

Remark 1: Generators are modeled as voltage sources [24] that are in series with equivalent resistors by Thévenin's Theorem. We assume that proper low-level controllers [2] have been employed to regulate the terminal voltage of a generator to track a reference setpoint. Consequently, the generator can automatically vary power outputs to respond to changing loading conditions. The generator internal dynamics, including those from low-level controllers and electromechanical transients, are not considered in this paper, and we mainly focus on the network dynamics contributed by electromagnetic transients in the stability analysis. Nevertheless, the main results of the paper can be extended to include various generator dynamics as well.

Remark 2: The main results of this paper can be extended to DC networks with other generator and load models. For example, constant-current and constant-impedance loads are linear and can be easily incorporated in the model. Additionally, for generators with V-I droop control [2], the voltage setpoint can be considered as the droop reference and the droop gains can be equivalently modeled as virtual impedances, which only changes the parameters of the RLC circuits.

2) Dynamic Network Model: Sources and loads are connected to DC buses. The buses form a connected graph where a bus is a node and an edge is a π-equivalent power line. For the p-th power line, let $i_{tp}(t)$ be the current flow and let R_{tp} and L_{tp} represent line resistance and inductance.

We exemplify the modeling approach using the circuit shown in Fig. 3. The state variables of the example circuit are the voltages of the capacitors and the currents through the inductors, namely, $v_{sk}(t)$, $v_{\ell j}(t)$, and $i_{tp}(t)$. The design variables are the output voltages of the sources, $V_k^{\text{ref}}, \forall k \in \mathcal{N}_s$. The dynamics of the circuit are represented by the following model using Kirchhoff's current and voltage laws,

$$\frac{di_{tp}(t)}{dt} = \frac{1}{L_{tp}} \left(v_{\ell j}(t) - R_{tp} i_{tp}(t) - v_{sk}(t)\right), \tag{1a}$$

$$\frac{dv_{sk}(t)}{dt} = \frac{1}{C_{sk}} \left(\frac{V_k^{\text{ref}} - v_{sk}(t)}{R_{sk}} + i_{to}(t) - i_{tk}(t)\right), \tag{1b}$$

$$\frac{dv_{\ell j}(t)}{dt} = \frac{1}{C_{\ell j}} \left(-\frac{v_{\ell j}(t)}{R_{\ell j}} - i_{td}(t) + i_{tk}(t) + \frac{p_{\ell j}}{v_{\ell j}(t)}\right). \tag{1c}$$

Equations (1a) and (1b) characterize the behavior of the power line and the source. They are linear in the state and design variables. However, (1c) is nonlinear due to the term, $p_{\ell j}/v_{\ell j}(t)$. Recall that $i_{to}(t)$ and $i_{td}(t)$ represent aggregate line currents flowing to the load and from the source, respectively, and they have similar dynamics to those of $i_{tp}(t)$.

The modeling approach can be applied to the entire system. By dropping the subscripts indicating variable indices, p_ℓ, v_ℓ, v_s, i_t, V^{ref} represent the vectors of load powers, load voltages, generator external voltages, power line currents, and controllable voltage setpoints, respectively. Let $x = [i_t^\top, v_s^\top, v_l^\top]^\top$ be the vector of state variables and $h(x, p_\ell) = [p_{\ell 1}/v_{\ell 1}, \cdots, p_{\ell n_\ell}/v_{\ell n_\ell}]^\top$.

With the above description and notation, the overall dynamics of the DC grid can be written as follows:

$$\dot{x}(t) = Ax(t) + BV^{\text{ref}} + Ch(x(t), p_\ell), \quad p_\ell \in \mathcal{P}_\ell, \tag{2}$$

where $A \in \mathbb{R}^{n \times n}$, $B \in \mathbb{R}^{n \times n_s}$, and $C \in \mathbb{R}^{n \times n_\ell}$ are constant matrices that are determined by the network topology and RLC circuit parameters through similar methods to those in [25]. This is a well-accepted model for DC network stability studies and has been applied to a variety of applications [2], [30], [31] (e.g., analyses of DC transmission system dynamics [30]).

Remark 3: So far, we have discussed a general model consisting of additive linear and nonlinear parts to represent the circuit dynamics. The model can be extended to represent control dynamics in a DC network as well. For example, secondary control for DC microgrids is usually designed using distributed averaging proportional-integral (DAPI) algorithms [32]. A DAPI control introduces a new additive linear

part into the system [33]. It is easy to augment system (2) to incorporate the control dynamics without changing the system structure. For the sake of simplicity, we omit control dynamics and derive our main results based on (2).

Let $X = [(I_t)^\top, (V_s)^\top, (V_\ell)^\top]^\top \in \mathbb{R}^n$ be an equilibrium of (2). When $V_{\ell k} \neq 0, \forall k \in \mathcal{N}_\ell$, the linearized Jacobian matrix of system (2) with respect to X is given as follows:

$$J(V_\ell, p_\ell) = A - \sum\nolimits_{k\in\mathcal{N}_\ell} \frac{p_{\ell k}}{V_{\ell k}^2} e_k e_k^\top, \tag{3}$$

where $e_k \in \mathbb{R}^n$ is a basis vector with the $(n_t + n_s + k)$-th element being $1/\sqrt{C_{\ell k}}$. The Jacobian matrix is an affine function in each term $p_{\ell k}/V_{\ell k}^2$. The form of this matrix shows that the local stability of an operating point depends on both the CPL power and the steady-state CPL voltage.

From basic control theory [34, Thm. 4.6], an equilibrium X of (2) is locally exponentially stable if there exists a real $n \times n$ positive definite matrix P that satisfies the following condition:

$$PJ(V_\ell, p_\ell) + J(V_\ell, p_\ell)^\top P \prec 0. \tag{4}$$

If p_ℓ and V_ℓ are given, this condition is a linear matrix inequality (LMI) constraint. However, in our problem, p_ℓ is uncertain, V_ℓ is unknown, and the coupling between V_ℓ and P is non-polynomial.

3) Power Flow Model: The power flow model describes the steady-state behavior at an operating point of a DC network. The power flow model is obtained by setting the left-hand side of (2) to $\mathbf{0}$ and rearranging terms as

$$p_\ell = \operatorname{diag}\{V_\ell\} \left(Y_{\ell\ell} V_\ell + Y_{\ell s} V^{\mathrm{ref}}\right), \tag{5}$$

where the connectivity between CPL–source and CPL–CPL are described by two admittance matrices $Y_{\ell s} \in \mathbb{R}^{n_\ell \times n_s}$ and $Y_{\ell\ell} \in \mathbb{R}^{n_\ell \times n_\ell}$ [35], which are submatrices of the system admittance matrix Y. Equation (5) is quadratic in state variables V_ℓ and bilinear in design variables V^{ref} and state variables V_ℓ. In general, the power flow model (5) usually introduces computational challenges owing to its non-convexity [6].

In addition, the system at steady state needs to satisfy operational constraints. In this paper, we require that $V_\ell \in \mathcal{V}_\ell$ and $V^{\mathrm{ref}} \in \mathcal{V}^{\mathrm{ref}}$. Both sets are convex sets that represent system operational requirements such as upper and lower voltage bounds. We limit our presentation to only consider the constraints related to the load voltages and generator setpoints, which are directly relevant to the system stability, in order to simplify the paper's discussion. Other variables like the currents are linear functions of the load voltages and generator voltage setpoints. The proposed algorithm can be easily extended to incorporate constraints on these variables.

C. Problem Statement

From the models discussed above, a poorly designed V^{ref} may 1) result in violations of operational constraints, 2) cause local instability for operating points, and 3) lead to infeasible solution to (5) or even loss of equilibrium altogether.

The goal of this work is to choose the value of V^{ref} which minimizes operating costs while guaranteeing that the system is robustly feasible and stable. We make the terms *robustly feasible* and *robustly stable* precise in Definition 1 below:

Definition 1: Given a generator voltage setpoint V^{ref}, system (2) is said to be *robustly feasible* if, for every $p_\ell \in \mathcal{P}_\ell$, the system admits an equilibrium X which satisfies all operational constraints. The system is said to be *robustly stable* if, for every $p_\ell \in \mathcal{P}_\ell$, there exists a corresponding V_ℓ such that the Jacobian $J(V_\ell, p_\ell)$ is Hurwitz.

Desirable operating points for power systems are usually computed by solving OPF problems [36]. Recently, OPF problems for DC networks (DN-OPF) have been a particular research focus [6]–[8], [13]. The formulation of existing DN-OPF problems can be summarized as follows:

$$\textbf{DN-OPF}^*\textbf{:} \quad \min f(V^{\mathrm{ref}}, V_\ell), \text{ subj. to} \tag{6a}$$
$$(5), \quad p_\ell = p_\ell^*, \tag{6b}$$
$$V_\ell \in \mathcal{V}_\ell, \quad V^{\mathrm{ref}} \in \mathcal{V}^{\mathrm{ref}}, \tag{6c}$$

where $p^* \in \mathbb{R}^{n_\ell}$ is the nominal CPL power profile and $f : \mathbb{R}^{n_s} \times \mathbb{R}^{n_\ell} \to \mathbb{R}$ is usually a convex cost function representing the operating cost (e.g., power loss or generation cost).

Note that our main results do not depend on the structure of the cost function. We therefore do not explicitly specify the cost functions in this paper in order to simplify our discussions. Our approach can easily accommodate typical OPF cost functions which depend on the operating point and generator setpoints. The illustrative case studies in Section IV consider the minimization of generation costs.

Recently, effective methods have been developed to solve the DN-OPF problem (6) using approximation and convex relaxation techniques [6]–[8], [13]. However, problem (6) only considers a fixed loading condition and does not explicitly consider system stability. If the actual load is different from the nominal load, the system's operating point may be unexpected and possibly even unstable.

To address these limitations, we focus on the following problem with explicit constraints guaranteeing robust feasibility and robust stability:

$$\textbf{R. DN-OPF SIP:} \quad \min f(V^{\mathrm{ref}}, V_\ell), \text{ subj. to} \tag{7a}$$
$$(4), \ (5), \ (6c), \quad \forall p_\ell \in \mathcal{P}_\ell. \tag{7b}$$

Compared to problem (6), we add the sufficient condition (4) in order to ensure stability. We also require all constraints to hold for all $p_\ell \in \mathcal{P}_\ell$ in order to ensure robust feasibility and robust stability in the presence of uncertainty.

Problem (7) is intractable in general due to the infinite number of constraints. Notice that problem (7) is a semi-infinite programming (SIP) problem [37]. Finding a tractable reformulation for the SIP problem (7) is challenging due to the nonlinearity and non-convexity of the stability condition (4) as well as the power flow equations (5).

III. Tractable DN-OPF with Robust Feasibility and Stability Guarantees

This section presents our algorithm to transform the computationally intractable problem (7) into a more amenable form. As illustrated in Fig. 1, the algorithm involves three

main steps: first, we formulate a computationally efficient optimization problem to find a stability set of V_ℓ that satisfies (4) for all $p_\ell \in \mathcal{P}_\ell$. Second, we develop a sufficient condition to show the existence of power flow solution V_ℓ in a set for any loading condition. Third, we develop a DN-OPF problem whose solution V^{ref} steers V_ℓ into the intersection of the stability set and operational constraint set.

A. Robust Stability Set

The stability set is the feasibility region of the stability condition (4). Due to the infinite number of constraints and the non-polynomial structure, this region is difficult to characterize. Motivated by power system operational constraints, this section describes an interval set which inner approximates this region.

Let $\underline{V}^s_{\ell j}$ and $\bar{V}^s_{\ell j} \in \mathbb{R}^{n_\ell}_+$ represent the lower and upper bounds of an interval set of V_ℓ, denoted as $\mathcal{V}^s_\ell = \left\{V_\ell : \underline{V}^s_{\ell j} \le V_{\ell j} \le \bar{V}^s_{\ell j}, \forall j \in \mathcal{N}_\ell\right\}$. We term $\mathcal{V}^s_\ell$ a "robust stability set" when the following definition applies:

Definition 2: A set $\mathcal{V}^s_\ell$ is called a *robust stability set* if there exists a positive definite matrix P such that the following inequality is satisfied for all $V_\ell \in \mathcal{V}^s_\ell$ and all $p_\ell \in \mathcal{P}_\ell$:

$$PJ\left(V_\ell, p_\ell\right) + J\left(V_\ell, p_\ell\right)^\top P \prec 0. \tag{8}$$

From this definition, any operating points lying in a robust stability set are stable regardless of the load profile. As shown below, this provides us with the flexibility to remove the coupling of equilibrium and load profiles.

1) Interpolation: The matrix $J(V_\ell, p_\ell)$ has the following two special structures: first, the unknown parameters $V_{\ell k}$ and $p_{\ell k}$ only exist in pairs on the diagonal entries in the form $-p_{\ell k}/V^2_{\ell k}$; second, each composite term $-p_{\ell k}/V^2_{\ell k}$ only appears once in the matrix. This provides the possibility of applying an interpolation method to replace each $-p_{\ell k}/V^2_{\ell k}$ with a new variable.

Let $\delta_k = -p_{\ell k}/V^2_{\ell k}$ and $\delta = [\delta_1, \cdots, \delta_{n_\ell}]^\top$. When $p_{\ell k}$ and $V_{\ell k}$ are subject to box constraints, the vector δ is contained in an interval set as well. Let $\Delta \triangleq \{\delta : \underline{\delta}_k \le \delta_k \le \bar{\delta}_k\}$ be such a constraint set.

With the above discussed definition, it can be easily checked that $J(\delta) = A + \sum_{k\in\mathcal{N}_\ell} \delta_k e_k^\top e_k$. Hence, the linearized system matrix is now subject to an affine interval parameter uncertainty. In the following, we denote this matrix as $J(\delta)$. We are interested in finding a Δ set for the unknown parameter that can always make the matrix Hurwitz stable, i.e., satisfy the following inequalities:

$$PJ(\delta) + J^\top(\delta)P \preceq 0, \quad \forall \delta \in \Delta. \tag{9}$$

Notice that once this Δ can be found, we can translate it into the desired robust stability set.

For a given Δ, there exist multiple methods to certify whether (9) is satisfied [1], [25]. Most existing methods check multiple "critical scenarios" to certify constraint satisfaction for all scenarios. The existing methods have issues with conservativeness or computational tractability. For example, the condition in [1] tests whether all diagonal elements of the Jacobian matrix are negative, which cannot be satisfied in our case when δ_j is positive. A sufficient condition based on LMI feasibility testing is proposed in [25] that involves 2^{n_ℓ} LMI constraints. While numerical tests reveal that the condition in [25] has advantages with respect to limited conservativeness, practical applicability of this condition is challenging since the number of LMI constraints is exponentially dependent on the dimension of the uncertainty.

TABLE I
VOLUME OF LARGEST CERTIFIABLE ROBUST STABILITY SET

	Lemma 1	Expo. LMIs [25]	Poly. LMIs [25]
Highest Load (kW)	-19.87	-19.96	-18.23

Notice that with our reformulation, the robust programming result in [37] can be applied to develop a new condition for DC network stability analysis:

Lemma 1: Given Δ, if there exists $P \succeq 0$, $N \preceq 0$, and n_ℓ positive scalars $\lambda_1, \cdots, \lambda_{n_\ell}$ that satisfy the following LMI conditions, $J(\delta)$ is always Hurwitz stable for all $\delta \in \Delta$:

$$\begin{bmatrix} N + \sum_{k=1}^{n_\ell} \lambda_k e_k e_k^\top \left(\frac{\bar{\delta}_k - \underline{\delta}_k}{2}\right)^2 & Pe_1 & \cdots & Pe_{n_\ell} \\ e_1^\top P & -\lambda_1 & & \\ \vdots & & \ddots & \\ e_{n_\ell}^\top P & & & -\lambda_{n_\ell} \end{bmatrix} \preceq 0, \tag{10a}$$

$$N \succeq P\left(A + \sum_{k=1}^{n_\ell} e_k e_k^\top \frac{\bar{\delta}_k + \underline{\delta}_k}{2}\right) + \left(A + \sum_{k=1}^{n_\ell} e_k e_k^\top \frac{\bar{\delta}_k + \underline{\delta}_k}{2}\right)^\top P. \tag{10b}$$

The condition in Lemma 1 only involves two LMIs. The decision variables are two $n \times n$ matrices, P and N, as well as n_ℓ scalars λ_j. In total, the condition has $2n^2 + n_\ell$ free scalar variables to select. Since this number is polynomially dependent on n and n_ℓ, the condition has reasonable tractability.

The reduction in computational complexity may induce concerns regarding conservativeness. One method to evaluate the conservativeness is to compare the volume of the largest sets that the conditions can certify. Compared to Lemma 1 of [25] where the number of LMIs is exponential in the number of loads, numerical tests show that the proposed conditions can certify a set with a volume above 95% of the largest set certifiable by exponentially many constraints. For example, we apply our results to the example DC microgrid detailed in Case Study 2 of [25]. The simulation results are shown in Table I. Notice that in the case study, we consider all pure-load buses and fix the voltage lower bounds, hence the volume of the stability set is indexed by the load power. Higher loads correspond to larger sets and a reduction in the condition's conservativeness. Note that the proposed results can certify a set with a volume over 99.5% relative to the condition with exponentially many LMIs in [25] and shows significant improvements compared to the condition with polynominally many LMIs in Proposition 1 of [25].

2) Computing the Robust Stability Set: With the proposed stability condition, we are equipped with a tractable method to check whether a given Δ satisfies (9). We would like to find a set Δ with a larger volume, as it can be translated into a robust stability set with a larger volume as well. The

volume of Δ is determined by its vertices, hence increasing the volume essentially involves adjusting these vertices. We use a line search method to accomplish this goal.

A subsequent question concerns selecting an initial guess for Δ that reduces computational efforts in finding a larger stability set. Rather than arbitrarily choosing an initial guess, we make one suggestion of the initial guess that may find the largest interval stability set in a single shot. This guess covers the entire domain of δ with respect to all possible power flow solutions. The details are provided in Appendix I.

With a slight abuse of notation, let the initial guess set be denoted as Δ. The volume of Δ can be adjusted by introducing a positive scaling factor α to all the vertices. We denote the set after adjustment as $\alpha\Delta$. We want to find the largest α that satisfies the condition of Lemma 1. This value is found by solving the following generalized eigenvalue problem (GEVP):

$$\textbf{GEVP:} \quad \max\ \alpha \quad \text{subj. to:} \tag{11a}$$

$$\begin{bmatrix} N+\alpha^2 \sum_{k=1}^{n_\ell} \lambda_k e_k e_k^\top \left(\frac{\bar{\delta}_k - \underline{\delta}_k}{2}\right)^2 & Pe_1 & \cdots & Pe_{n_\ell} \\ e_1^\top P & -\lambda_1 & & \\ \vdots & & \ddots & \\ e_{n_\ell}^\top P & & & -\lambda_{n_\ell} \end{bmatrix} \preceq 0, \tag{11b}$$

$$N \preceq 0, P \succeq 0, \alpha > 0, \ \text{(10b)}.$$

A solution that is arbitrarily close to the global optimum can be found for the GEVP problem (11) since it is a quasi-convex problem [38]. For a solution α of (11), we are endowed with a robust stability set as described below.

Proposition 1: Given Δ, if α is a solution of (11), $\mathcal{V}_\ell^s$ defined in the following is a robust stability set:

$$\mathcal{V}_\ell^s = \{V_\ell : V_{\ell k} \geq \delta_k^{\max}, \forall k \in \mathcal{N}_\ell\},$$

where $\delta_k^{\max} = \max\{-\bar{p}_{\ell k}/(\alpha \underline{\delta}_k), -\underline{p}_{\ell k}/(\alpha \bar{\delta}_k)\}$.

In Proposition 1, we find the lower bound for the steady-state voltage to ensure robust stability. This bound is in line with engineering observations for DC grid stability: with larger load power, the system should be operated at higher voltage levels to reduce risks of instability.

Remark 4: The value of α is critical for determining the robust stability set. As the set includes all relevant uncertainty realizations, we do not need to test if the system is stable for uncertainty outside of the set. Thus, the value of α is upper bounded by 1. When the solution is obtained as 1, the largest interval stability set can be directly found. Otherwise, a line search algorithm can be developed to approximately solve (11).

B. Solvability Condition

As shown in Fig. 1, when the robust stability set is found our next task is to ensure: a) the system operates in this set and b) the system complies with all other operational constraints. This task is equivalent to the following robust feasibility problem: we need to compute a voltage setpoint $V^{\text{ref}} \in \mathcal{V}^{\text{ref}}$ that guarantees the existence of power flow solutions (i.e., solutions to (5)) that are in $\mathcal{V}_\ell^s \cap \mathcal{V}_\ell^e$ for all $p_\ell \in \mathcal{P}_\ell$.

We first present a new solvability condition which characterizes the variations of operating points for given generator setpoints. The main ingredient is a novel "convex restriction" (i.e., a convex set within the non-convex set of feasible operating points) that is tailored for DC networks. Related work in [39] formulates convex restrictions for general AC OPF problems. We show that an analogous convex restriction can be derived for DC grids with known interval uncertainties.

To facilitate our discussion, we rearrange (5) into the following fixed-point form:

$$V_\ell = F(V_\ell; p_\ell) \triangleq E + Z_{\ell\ell}\, \text{diag}\{p_\ell\} r(V_\ell), \tag{12}$$

where we denote $Z_{\ell\ell} = Y_{\ell\ell}^{-1}$, $E = -Y_{\ell\ell}^{-1} Y_{\ell s} V^{\text{ref}}$, and $r(V_\ell) = [1/V_{\ell 1}, \cdots, 1/V_{\ell n_\ell}]^\top$ yields the element-wise reciprocal of vector V_ℓ.

Based on the fixed-point form (12), we show the existence and boundaries of power flow solutions for any loading condition $p_\ell \in \mathcal{P}_\ell$ when the power flow solutions for the extreme loading conditions are known.

Lemma 2: If $V_{\ell -} > \mathbf{0}$ is a fixed point of $F(\cdot\,; \underline{p}_\ell)$ for a given V^{ref}, then there exists $V_\ell \geq V_{\ell -}$ that satisfies $V_\ell = F(V_\ell; p_\ell)$ for all $p_\ell \in [\underline{p}_\ell, \bar{p}_\ell]$.

Proof: Available in Appendix II. ■

Lemma 2 describes a power flow solution existence condition which states that operating points exist for all $p_\ell \in [\underline{p}_\ell, \bar{p}_\ell]$ as long as the power flow equations are solvable at the high-loading condition. In addition, this condition shows that the high-loading solution is a lower bound on these operating points. The next result derives an upper bound on the operating points based on another extreme scenario, i.e., the low-loading solution.

Proposition 2: If $V_{\ell -} > \mathbf{0}$ is a fixed point of $F(\cdot; \underline{p}_\ell)$ for given V^{ref} and the following inequality holds:

$$||Z_{\ell\ell}\, \bar{p}_\ell\ \text{diag}\{r(E)\}\, r(E)|| < 1,$$

then there exists $V_\ell \in [V_{\ell -}, V_{\ell +}]$ that satisfies $V_\ell = F(V_\ell; p_\ell)$ for any $p_\ell \in [\underline{p}_\ell, \bar{p}_\ell]$, where $V_{\ell +}$ is a unique fixed point of $F(\cdot\,; \bar{p}_\ell)$ in $[E, +\infty)$.

Proof: Available in Appendix III. ■

Proposition 2 shows the existence of operating points in a box constraint, where the upper bound is the high-voltage solution at the low-loading condition. Along with Lemma 2, Proposition 2 provides the following two implications that align with engineering observations:

1. (*Existence*) We only need to verify that the system is solvable at the high-loading condition to ascertain the solvability of all the other circumstances.
2. (*Monotonicity*) The high- and low-loading solutions jointly define a solution range, where the high-loading solution provides bounds from below and low-loading solution provides bounds from above.

These implications can help reduce computational efforts in DC network operations. For example, one only needs to examine whether the system has an operating point in the high-loading condition to certify all the other cases. Moreover, these conditions are key for developing a solution algorithm for (7).

C. Robust DN-OPF

As we have characterized a cluster of operating points with respect to given generator setpoints, the remaining task is to design the setpoints to steer the cluster into the desired set (i.e., $\mathcal{V}_\ell^s \cap \mathcal{V}_\ell^e$) and to reduce system operational costs.

To accomplish these two objectives, an optimization problem can be formulated as

$$\textbf{R. DN-OPF*:}\ \min\ f(V^{\mathrm{ref}}, V_{\ell-}, V_{\ell+})\ \text{subj. to} \tag{13a}$$
$$\underline{p}_\ell = \mathrm{diag}\{V_{\ell-}\}\left(Y_{\ell\ell}\, V_{\ell-} + Y_{\ell s}\, V^{\mathrm{ref}}\right), \tag{13b}$$
$$\bar{p}_\ell = \mathrm{diag}\{V_{\ell+}\}\left(Y_{\ell\ell}\, V_{\ell+} + Y_{\ell s}\, V^{\mathrm{ref}}\right), \tag{13c}$$
$$E = -Z_{\ell\ell}\, Y_{\ell s}\, V^{\mathrm{ref}}, \tag{13d}$$
$$s\mathbf{1} \le E, \quad s^2 \ge Z_{\ell\ell}\, \bar{p}_\ell,\ s > 0, \tag{13e}$$
$$E \le V_{\ell+}, \tag{13f}$$
$$V_{\ell-} \in \mathcal{V}_\ell^s \cap \mathcal{V}_\ell^e, \quad V_{\ell+} \in \mathcal{V}_\ell^s \cap \mathcal{V}_\ell^e, \tag{13g}$$
$$V^{\mathrm{ref}} \in \mathcal{V}^{\mathrm{ref}}, \tag{13h}$$

where s is a positive scalar slack variable. Constraints (13b) and (13c) represent the DN power flow equations for the high- and low-loading conditions, constraints (13d)–(13f) enforce the condition of Proposition 2, and constraints (13g)–(13h) ensure the operating points are steered into the desired set.

A solution of (13) yields generator setpoints which ensure robust stability and feasibility, as stated by the following result:

Theorem 1: Any solution of (13) is a feasible point of (7).

Proof: Available in Appendix IV. ∎

Theorem 1 shows that the feasibility of (13) implies the feasibility of (7). Problem (13) only contains linear and quadratic constraints whose structure resembles that of a classic DN-OPF problem (6). Thus, existing DN-OPF algorithms can be leveraged to solve (13). We use the following algorithm to summarize the main result of the paper:

Algorithm 1 Find V^{ref} for SIP (7)

Input: System matrices A, B, C, D, load uncertainty set $\mathcal{P}_\ell$, constraint sets $\mathcal{V}_\ell^e$ and $\mathcal{V}^{\mathrm{ref}}$.
Output: A solution V^{ref}.

Step 1: Solve (14) in Appendix I to find individual steady-state voltage lower bound $V_{\ell k-}^2$, for all $k \in \mathcal{N}_\ell$.
Step 2: Construct Δ.
Step 3: Solve GEVP (11) to find α and all $\delta_k^{\max}, k \in \mathcal{N}_\ell$.
Step 4: Find robust stability set $\mathcal{V}_\ell^s$.
Step 5: Solve problem (13) to find V^{ref}.

Using Algorithm 1, we can compute generator setpoints that ensure robust stability and feasibility. As previously discussed, the algorithm can be executed efficiently with existing tools.

Remark 5 (Actual Operating Points): Our work can ensure the robust stability and feasibility of the actual operating points. Like a general power system, a DC network usually operates at a high-voltage power flow solution [40]. As discussed in Appendix III, all high-voltage solutions are bounded from above by that of the low-loading condition and from below by that of the high-loading condition. Note that $V_{\ell+}$ is the high-voltage solution at the low-loading condition, hence it is a tight upper bound for the system's high-voltage solutions. In addition, $V_{\ell-}$ is a solution at the high-loading condition, which is element-wise less than or equal to the high-is solution. Hence, any high-voltage solution must reside in the range $[V_{\ell-}, V_{\ell+}]$, which is entirely steered into the desired set.

Remark 6 (Conservativeness): Numerical studies show that the proposed approach has limited conservativeness. First, as discussed in Section III-A the stability condition has limited conservativeness. Second, numerical studies suggest that the interval bound $[V_{\ell-}, V_{\ell+}]$ usually has no gap with respect to the actual operating point variation range.

TABLE II
PARAMETERS FOR THE 14-BUS DC NETWORK CASE STUDY

R_{sk}	0.05 Ω	R_{lj}	5 Ω	R_{tp}	0.05 Ω
L_{tp}	3mH	C_{sk}	0.75mF	C_{lj}	0.9mF

IV. Case Studies

This section demonstrates the effectiveness of the proposed algorithm using simulation case studies. The optimization problems are solved using IPOPT [41], and the simulations are performed in Matlab/Simulink. We first show the efficacy and the limited conservativeness of the proposed work with a 14-bus system. We then demonstrate the computational efficiency of the proposed approach.

A. Efficacy and Conservativeness

We first focus on an example DC network whose topology and bus types are the same as the IEEE 14-bus system. The parameters of the DC network given in Table II are chosen according to existing DC network case studies [35], [42].

For this example system, we assume all the loads are constant power components. We consider three scenarios: 1) all load case, where power outputs of each constant power component varies in $[-50\ \mathrm{kW}, 0]$; 2) all generation case, where power outputs of each constant power component varies in $[0, 50\ \mathrm{kW}]$; and 3) all mixed case, where each constant power component varies in $[-50\ \mathrm{kW}, 50\ \mathrm{kW}]$.

We use the first scenario to demonstrate that the generator setpoints designed using our results ensure robust stability and feasibility. For this case study, we impose operational bounds of $[450\ \mathrm{V}, 550\ \mathrm{V}]$ on the generator and CPL voltages, which allows a ± 0.1 p.u. deviation when 500 V is set as base voltage. The objective function minimizes the generation costs at the nominal operating condition, which is set to be 25 kW.

When we ignore the range of possible uncertainty realizations, the solution to the DN-OPF problem (6) yields setpoints of the five generators as $[481.8, 489.7, 481.2, 480.6, 486.5]$ V. We apply these setpoints and consider a uniform increase in load demands of 2.5 kW every 2.5 seconds. As shown in Fig. 4, the system becomes unstable at approximately 40 seconds when the loads are around 45 kW. In the zoomed-in figure, one can see that by approximately 38 seconds, the system is already in an oscillatory state. This shows the need to consider stability properties for operating point design, especially in systems with significant uncertainties.

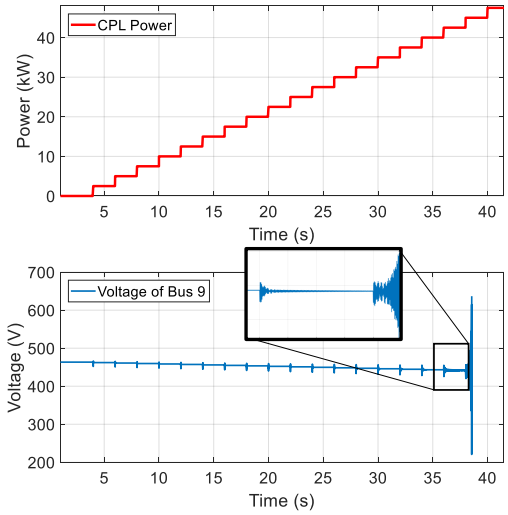

Fig. 4. DC network instability if only the nominal loading condition is considered.

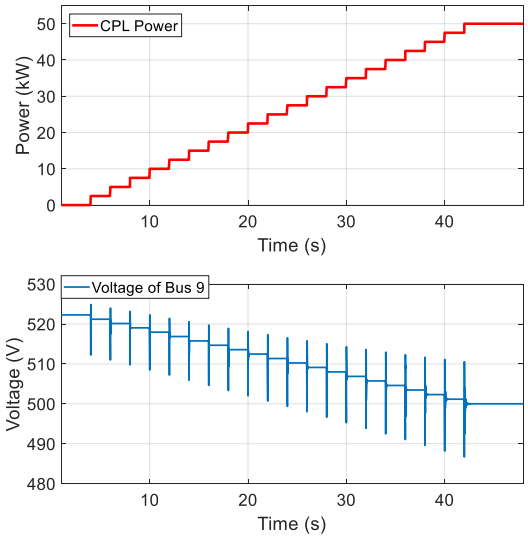

Fig. 5. DC network operation is stable for all conditions using the proposed algorithm.

In comparison, we formulate the optimization problem (13) using our algorithm. Applying the stability analysis approach developed in Section III-A shows that the system is always robustly stable if the steady-state CPL voltage is higher than 500 V. Problem (13) yields the following setpoints: $[543.5, 550.0, 542.8, 542.1, 549.3]$ V. Using these setpoints results in robust stability for the entire range of load demands, as empirically corroborated by Fig. 5. Observe that the system remains stable when the loads are increased at the same rate as in the previous test.

Moreover, we show that our approach can recover the exact power flow solution variation range. Table III presents the difference of the obtained $[V_{\ell-}, V_{\ell+}]$ relative to the actual lower and upper bounds observed in the simulation for the three scenarios. Observe that we find the exact variation range of the system's actual operating points. This demonstrates the limited conservativeness of the proposed algorithm.

TABLE III
ERROR FOR OPERATING POINT BOUNDS

	All gen.	All loads	All mixed
Error for upper bound	0	0	0
Error for lower bound	0	0	0

TABLE IV
COMPARISON OF COMPUTATION TIMES FOR SOLVING (6) AND (13)

	9-bus	39-bus	118-bus	300-bus	2383-bus
DN-OPF (6)	0.04 s	0.09 s	0.17 s	0.26 s	0.87 s
Problem (13)	0.08 s	0.16 s	0.50 s	1.77 s	196.21 s

B. Computational Efficiency

We have tested the computational tractability of DN-OPF problem (13) on DC networks with the same topology and bus types as the IEEE 9-, 39-, 118-, 300-, and 2383-bus systems. To summarize the results, Table IV compares the average CPU time in IPOPT for solving problem (13) and the traditional DN-OPF problem (6), averaged over 10 tests for each system. Observe that the proposed optimization problem has a similar computational complexity as the traditional DN-OPF problem for systems with moderate sizes, and is still reasonably tractable for large-scale systems like 2383-bus system. This verifies the tractability of our algorithm.

V. CONCLUSION

This paper has developed an algorithm for solving stability-constrained OPF problems in DC networks under uncertainty. Such problems are usually intractable due to infinitely many constraints. Our algorithm uses computationally efficient approaches to transform the problem into a tractable counterpart that resembles a traditional DN-OPF problem such that existing tools can be employed. We first derive a robust stability set within which any operating point is guaranteed to be robustly stable. We then use a sufficient condition which ensures the existence of feasible operating points in this set for all uncertainty realizations in the specified uncertainty set. Low conservativeness and high computational efficiency of the proposed algorithm are demonstrated using various test cases. In future research, we will investigate the application of the algorithm to DN-OPF problems with contingency constraints.

APPENDIX I
SUGGESTED INITIAL GUESS FOR ROBUST STABILITY SET

The suggested set is motivated by the outer convex approximation of an OPF problem. The main idea is to find an outer approximation of the domain of δ. To find a tight approximation, we look into the coupling between p_ℓ and V_ℓ^2 since they constitute δ.

For different power flow solutions and power profiles, the value of δ varies. Let δ_{k+} and δ_{k-} be the upper and lower boundaries for δ_k. In addition, we use $V_{\ell k+}^2$ and $V_{\ell k-}^2$ to represent a pair of upper and lower bounds of V_ℓ^2 for any feasible solution.

The values of δ_{j-} and δ_{j+} can be determined based on the loading condition at bus j:

- pure generation bus, i.e., when $0 \le \underline{p}_{\ell j} \le \bar{p}_{\ell j}$, $\delta_{j+} = -\underline{p}_{\ell j}/V_{\ell j+}^2$ and $\delta_{\ell j-} = -\bar{p}_{\ell j}/V_{\ell j-}^2$;
- pure load bus, i.e., when $\underline{p}_{\ell j} \le \bar{p}_{\ell j} \le 0$, $\delta_{\ell j+} = -\underline{p}_{\ell j}/V_{\ell j-}^2$ and $\delta_{\ell j-} = -\bar{p}_{\ell j}/V_{\ell j+}^2$; and
- mixed bus, i.e., when $\underline{p}_{\ell j} \le 0 \le \bar{p}_{\ell j}$, $\delta_{\ell j+} = -\underline{p}_{\ell j}/V_{\ell j-}^2$ and $\delta_{\ell j-} = -\bar{p}_{\ell j}/V_{\ell j-}^2$.

As discussed in Section II-B, we assume that all the buses in $\mathcal{N}_\ell$ are mixed buses in order to simplify our discussion, but our results can be easily extended to the other two types.

With mixed buses, we only need to find $V_{\ell k-}^2$ in order to obtain δ_{k+} and δ_{k-}. Such a bound can be found through solving the following problem:

$$\textbf{Lower Bound:} \quad \min V_{\ell k}^2, \ \text{subj. to} \tag{14a}$$

$$(5),\ (6c),\ p_\ell \in \mathcal{P}_\ell. \tag{14b}$$

Notice that (14) is a conventional optimal power flow problem with a QCQP formulation. Since we only need to find a lower bound on the steady-state voltage, one can apply a second-order cone programming (SOCP) relaxation method to find a lower bound of the global optimum of (14).[1]

With lower bounds found, each pair of δ_{k-} and δ_{k+} can be obtained. They form the vertices of the initial guess for Δ. This set includes any realization of δ that follows the DC network physics and operational constraints.

APPENDIX II
PROOF OF LEMMA 2

Proof: To establish the argument, we apply Brouwer's fixed-point theorem, which states that for any continuous function F mapping a compact convex set to itself there is a point x_0 in the set such that $F(x_0) = x_0$.

We seek to show that $[V_{\ell-},\, F(V_{\ell-};\, \bar{p}_\ell)]$ is an invariant set for any $F(\cdot;\, p_\ell)$ with $p_\ell \in \mathcal{P}_\ell$.

We first show the interval $[V_{\ell-}, F(V_{\ell-};\, \bar{p}_\ell)]$ is well-defined. Notice that $F(V_\ell;\, p_\ell) = E + Z_{\ell\ell}\, p_\ell\, r(V_\ell)$, where the first term on the right-hand side is a constant for given $V^{\rm ref}$ and $Z_{\ell\ell}$ is a positive matrix as its inverse $Y_{\ell\ell}$ is an M-matrix. As a result, for given $V_\ell > \mathbf{0}$, each element of $F(V_\ell;\, p_\ell)$ is a monotonically increasing function in each element of p_ℓ. As $\bar{p}_\ell \ge \underline{p}_\ell$, $V_{\ell-} = F(V_{\ell-};\, \underline{p}_\ell) \le F(V_{\ell-};\, \bar{p}_\ell)$.

Next, we show that $F(\cdot;\, p_\ell)$ maps $[V_{\ell-}, F(V_{\ell-};\, \bar{p}_\ell)]$ to itself. Notice that $\underline{p}_\ell \le \mathbf{0} \le \bar{p}_\ell$, $F(V_\ell;\, \underline{p}_\ell)$ is monotonically increasing in each element of V_ℓ and $F(V_\ell;\, \bar{p}_\ell)$ is monotonically decreasing in each element of V_ℓ. For an arbitrary $V_\ell \in [V_{\ell-}, F(V_{\ell-};\, \bar{p}_\ell)]$, we can lower and upper bound $F(V_\ell;\, p_\ell)$ by

$$V_{\ell-} \le F(V_\ell;\, \underline{p}_\ell) \le F(V_\ell;\, p_\ell) \le F(V_\ell;\, \bar{p}_\ell) \le F(V_{\ell-};\, \bar{p}_\ell) \tag{15}$$

From (15), Brouwer's fixed-point theorem can be applied to complete the proof. ■

[1] With certain conditions on problem structure, the SOCP relaxation of (14) is exact. Detailed discussion can be found in [6], [7].

APPENDIX III
PROOF OF PROPOSITION 2

Proof: Banach's fixed-point theorem is used to establish the proof. It states that for any contraction mapping F on a complete metric space mapping a set to itself, there is a unique point x_0 in the set such that $F(x_0) = x_0$.

We seek to show that all system operating points are upper bounded by the high-voltage solution of the low-loading condition. Denote the high-voltage solution of a fixed-point function $F(\,\cdot\,;\, p_\ell)$ by $F_{p_\ell}^{\max}$ with the following definition: a fixed point $F_{p_\ell}^{\max}$ is called a high-voltage solution of $F(\,\cdot\,;\, p_\ell)$ if $V_\ell \le F_{p_\ell}^{\max}$ for any fixed point $V_\ell \in \mathbb{R}^{n_\ell}$. It follows from [43] that $F_{p_\ell}^{\max}$ exists and for any p^a and p^b such that $\underline{p}_\ell \le p^a \le p^b \le \bar{p}_\ell$, the high-voltage solution has the following monotonicity: $F_{p^a}^{\max} \le F_{p^b}^{\max}$. Consequently, $F_{\underline{p}_\ell}^{\max} \le F_{p_\ell}^{\max} \le F_{\bar{p}_\ell}^{\max}$ for any $p_\ell \in \mathcal{P}_\ell$.

Then, we show that $F(\,\cdot\,;\, \bar{p}_\ell)$ is a self map on $[E, +\infty)$. Notice that $E > 0$, and $F(\,\cdot\,;\, \bar{p}_\ell) = E + Z_{\ell\ell}\, \bar{p}_\ell\, r(V_\ell)$ with positive matrix $Z_{\ell\ell}$ and non-negative $\bar{p}_\ell$. Hence, the second term on the right-hand side must be non-negative. Thus, for all $V_\ell \in [E, +\infty)$ we have $F(V_\ell;\, \bar{p}_\ell) \ge E$.

Next, we show that $F(\,\cdot\,;\, \bar{p}_\ell)$ is a contraction mapping on $[E, +\infty)$. For any $V^a, V^b \in [E, +\infty)$, the Euclidean norm of $F(V^a;\, \bar{p}_\ell) - F(V^b;\, \bar{p}_\ell)$ is upper bounded as follows

$$\begin{aligned} ||F(V^a;\, \bar{p}_\ell) - F(V^b;\, \bar{p}_\ell)|| &= ||Z_{\ell\ell}\, \bar{p}_\ell \left(r(V^a) - r(V^b)\right)|| \\ &\le ||Z_{\ell\ell}\, \bar{p}_\ell\ \mathrm{diag}\{r(E)\}\, r(E)||\,||V^a - V^b||, \end{aligned} \tag{16}$$

where $||Z_{\ell\ell}\, \bar{p}_\ell\ \mathrm{diag}\{r(E)\}\, r(E)||$ is a positive constant less than 1. Hence, $F(\cdot;\, \bar{p}_\ell)$ is a contraction mapping on $[E, +\infty)$.

From the Banach fixed-point theorem, $F(\,\cdot\,;\, \bar{p}_\ell)$ has a unique fixed point $V_{\ell+}$ in $[E, +\infty)$. Obviously, it is the high-voltage solution of the low-loading condition. Consequently, it bounds the high-voltage solutions of all loading conditions from above, i.e., for any $p_\ell \in \mathcal{P}_\ell$, we have $V_{\ell+} \ge F_{p_\ell}^{\max}$.

Lemma 2 implies that there exist high-voltage solutions $F_{p_\ell}^{\max}$ that are lower bounded by $V_{\ell-}$ for all $p_\ell \in \mathcal{P}_\ell$. Together with inequality $V_{\ell+} \ge F_{p_\ell}^{\max}$, the high-voltage solutions lie in box constraint $[V_{\ell-}, V_{\ell+}]$. ■

APPENDIX IV
PROOF OF THEOREM 1

Proof: Suppose $V^{\rm ref}$, $V_{\ell-}$, $V_{\ell+}$, and s are solutions of (13). We only need to show $V^{\rm ref}$ ensures robust stability and robust feasibility as defined in Definition 1.

First, when (13) is feasible, the condition of Proposition 2 is satisfied since constraints (13b)–(13f) hold. Proposition 2 says that $F(\,\cdot\,;\, p_\ell)$ defined in (12) must have a fixed point V_ℓ in $[V_{\ell-},\, V_{\ell+}]$ for any $p_\ell \in [\underline{p}_\ell,\, \bar{p}_\ell]$. In other words, the power flow equations (5) always have a solution in $[V_{\ell-},\, V_{\ell+}]$.

Second, from (13g) the interval $[V_{\ell-},\, V_{\ell+}]$ belongs to $\mathcal{V}_\ell^s \cap \mathcal{V}_\ell^e$. Hence, the fixed point $V_\ell \in \mathcal{V}_\ell^s \cap \mathcal{V}_\ell^e$ as well. Thus, the system power flow solution satisfies both the operational constraints and the stability constraints.

Since $V_\ell \in \mathcal{V}_\ell^e$ and $V^{\rm ref} \in \mathcal{V}^{\rm ref}$, the system is robustly feasible. Since $V_\ell \in \mathcal{V}_\ell^s$, by Proposition 1 the system is also robustly stable. Thus, the proof is complete. ■

REFERENCES

[1] F. Dörfler, J. W. Simpson-Porco, and F. Bullo, "Electrical networks and algebraic graph theory: Models, properties, and applications," *Proceedings of the IEEE*, vol. 106, no. 5, pp. 977–1005, 2018.

[2] T. Dragičević, X. Lu, J. C. Vasquez, and J. M. Guerrero, "DC microgrids—Part I: A review of control strategies and stabilization techniques," *IEEE Transactions on Power Electronics*, vol. 31, no. 7, pp. 4876–4891, 2016.

[3] K. Lehmann, A. Grastien, and P. Van Hentenryck, "AC-feasibility on tree networks is NP-hard," *IEEE Transactions on Power Systems*, vol. 31, no. 1, pp. 798–801, 2016.

[4] D. K. Molzahn and I. A. Hiskens, "A survey of relaxations and approximations of the power flow equations," *Foundations and Trends in Electric Energy Systems*, vol. 4, no. 1-2, pp. 1–221, Feb. 2019.

[5] M. Farasat, S. Mehraeen, A. Arabali, and A. Trzynadlowski, "GA-based optimal power flow for microgrids with DC distribution network," in *IEEE Energy Conversion Congress and Exposition (ECCE)*, 2015, pp. 3372–3379.

[6] L. Gan and S. H. Low, "Optimal power flow in direct current networks," *IEEE Transactions on Power Systems*, vol. 29, no. 6, pp. 2892–2904, 2014.

[7] J. Li, F. Liu, Z. Wang, S. H. Low, and S. Mei, "Optimal power flow in stand-alone DC microgrids," *IEEE Transactions on Power Systems*, vol. 33, no. 5, pp. 5496–5506, 2018.

[8] O. D. Montoya, W. Gil-González, and A. Garcés, "Optimal power flow on DC microgrids: A quadratic convex approximation," *IEEE Transactions on Circuits and Systems II: Express Briefs*, pp. 1–1, 2018.

[9] A. Garcés, "On the convergence of Newton's method in power flow studies for DC microgrids," *IEEE Transactions on Power Systems*, vol. 33, no. 5, pp. 5770–5777, Sept. 2018.

[10] W. Inam, J. A. Belk, K. Turitsyn, and D. J. Perreault, "Stability, control, and power flow in ad hoc DC microgrids," in *17th IEEE Workshop on Control and Modeling for Power Electronics (COMPEL)*, 2016, pp. 1–8.

[11] J. Ma, L. Yuan, Z. Zhao, and F. He, "Transmission loss optimization-based optimal power flow strategy by hierarchical control for DC microgrids," *IEEE Transactions on Power Electronics*, vol. 32, no. 3, pp. 1952–1963, Mar. 2017.

[12] B. Stott, J. Jardim, and O. Alsaç, "DC power flow revisited," *IEEE Transactions on Power Systems*, vol. 24, no. 3, pp. 1290–1300, 2009.

[13] O. D. Montoya, L. Grisales-Norena, D. González-Montoya, C. Ramos-Paja, and A. Garcés, "Linear power flow formulation for low-voltage DC power grids," *Electric Power Systems Research*, vol. 163, pp. 375–381, 2018.

[14] F. Cingoz, A. Elrayyah, and Y. Sozer, "Optimized settings of droop parameters using stochastic load modeling for effective DC microgrids operation," *IEEE Transactions on Industrial Applications*, vol. 53, no. 2, pp. 1358–1371, Mar. 2017.

[15] R. Louca and E. Bitar, "Robust AC optimal power flow," *IEEE Transactions on Power Systems*, vol. 34, no. 3, pp. 1669–1681, May 2019.

[16] D. K. Molzahn and L. A. Roald, "Towards an AC optimal power flow algorithm with robust feasibility guarantees," in *Power Systems Computation Conference (PSCC)*, 2018, pp. 1–7.

[17] J. W. Simpson-Porco, F. Dörfler, and F. Bullo, "Voltage collapse in complex power grids," *Nature Communications*, vol. 7, p. 10790, 2016.

[18] B. Cui and X. A. Sun, "A new voltage stability-constrained optimal power-flow model: Sufficient condition, SOCP representation, and relaxation," *IEEE Transactions on Power Systems*, vol. 33, no. 5, pp. 5092–5102, Sept. 2018.

[19] A. P. N. Tahim *et al.*, "Modeling and stability analysis of islanded DC microgrids under droop control," *IEEE Transactions on Power Electronics*, vol. 30, no. 8, pp. 4597–4607, Aug. 2015.

[20] N. Barabanov, R. Ortega, R. Gri, and B. Polyak, "On existence and stability of equilibria of linear time-invariant systems with constant power loads," *IEEE Transactions on Circuits and Systems I: Regular Papers*, vol. 63, no. 1, pp. 114–121, Jan. 2016.

[21] L. Herrera, W. Zhang, and J. Wang, "Stability analysis and controller design of DC microgrids with constant power loads," *IEEE Transactions on Smart Grid*, vol. 8, no. 2, pp. 881–888, Mar. 2017.

[22] D. Marx, P. Magne, B. Nahid-Mobarakeh, S. Pierfederici, and B. Davat, "Large signal stability analysis tools in DC power systems with constant power loads and variable power loads—A review," *IEEE Transactions on Power Electronics*, vol. 27, no. 4, pp. 1773–1787, April 2012.

[23] D. Zonetti, R. Ortega, and J. Schiffer, "A tool for stability and power-sharing analysis of a generalized class of droop controllers for high-voltage direct-current transmission systems," *IEEE Transactions on Control of Network Systems*, vol. 5, no. 3, pp. 1110–1119, Sept. 2018.

[24] J. A. Belk, W. Inam, D. J. Perreault, and K. Turitsyn, "Stability and control of ad hoc DC microgrids," in *IEEE 55th Annual Conference on Decision and Control (CDC)*, Dec. 2016, pp. 3271–3278.

[25] J. Liu, W. Zhang, and G. Rizzoni, "Robust stability analysis of DC microgrids with constant power loads," *IEEE Transactions on Power Systems*, vol. 33, no. 1, pp. 851–860, Jan. 2018.

[26] R. Hettich and K. O. Kortanek, "Semi-infinite programming: Theory, methods, and applications," *SIAM Review*, vol. 35, no. 3, pp. 380–429, 1993.

[27] J. M. Mulvey, R. J. Vanderbei, and S. A. Zenios, "Robust optimization of large-scale systems," *Operations Research*, vol. 43, no. 2, pp. 264–281, 1995.

[28] A. Ben-Tal, L. El Ghaoui, and A. Nemirovski, *Robust Optimization*. Princeton University Press, 2009, vol. 28.

[29] N. Bottrell, M. Prodanovic, and T. C. Green, "Dynamic stability of a microgrid with an active load," *IEEE Transactions on Power Electronics*, vol. 28, no. 11, pp. 5107–5119, Nov. 2013.

[30] G. O. Kalcon, G. P. Adam, O. Anaya-Lara, S. Lo, and K. Uhlen, "Small-signal stability analysis of multi-terminal VSC-based DC transmission systems," *IEEE Transactions on Power Systems*, vol. 27, no. 4, pp. 1818–1830, Nov. 2012.

[31] A. Emadi, A. Khaligh, C. H. Rivetta, and G. A. Williamson, "Constant power loads and negative impedance instability in automotive systems: Definition, modeling, stability, and control of power electronic converters and motor drives," *IEEE Transactions on Vehicular Technology*, vol. 55, no. 4, pp. 1112–1125, July 2006.

[32] D. K. Molzahn, F. Dörfler, H. Sandberg, S. H. Low, S. Chakrabarti, R. Baldick, and J. Lavaei, "A survey of distributed optimization and control algorithms for electric power systems," *IEEE Transactions on Smart Grid*, vol. 8, no. 6, pp. 2941–2962, Nov. 2017.

[33] T. Morstyn, B. Hredzak, G. D. Demetriades, and V. G. Agelidis, "Unified distributed control for dc microgrid operating modes," *IEEE Transactions on Power Systems*, vol. 31, no. 1, pp. 802–812, Jan. 2016.

[34] H. K. Khalil, *Nonlinear Systems*, 3rd ed. Upper Saddle River, NJ: Prentice Hall, 2002.

[35] Z. Liu, M. Su, Y. Sun, W. Yuan, H. Han, and J. Feng, "Existence and stability of equilibrium of DC microgrid with constant power loads," *IEEE Transactions on Power Systems*, vol. 33, no. 6, pp. 6999–7010, Nov. 2018.

[36] M. B. Cain, R. P. O'Neill, and A. Castillo, "History of optimal power flow and formulations (OPF paper 1)," *US Federal Energy Regulatory Commission*, pp. 1–36, 2012.

[37] A. Ben-Tal and A. Nemirovski, "Robust optimization—Methodology and applications," *Mathematical Programming*, vol. 92, no. 3, pp. 453–480, 2002.

[38] S. Boyd and L. Vandenberghe, *Convex Optimization*. Cambridge University Press, 2004.

[39] D. Lee, H. D. Nguyen, K. Dvijotham, and K. Turitsyn, "Convex restriction of power flow feasibility sets," *IEEE Transactions on Control of Network Systems*, vol. 6, no. 3, pp. 1235–1245, Sept. 2019.

[40] J. W. Simpson-Porco, F. Dörfler, and F. Bullo, "On resistive networks of constant-power devices," *IEEE Transactions on Circuits and Systems II: Express Briefs*, vol. 62, no. 8, pp. 811–815, Aug. 2015.

[41] A. Wächter and L. T. Biegler, "On the implementation of an interior-point filter line-search algorithm for large-scale nonlinear programming," *Mathematical Programming*, vol. 106, no. 1, pp. 25–57, Mar. 2006.

[42] D. Salomonsson and A. Sannino, "Low-voltage DC distribution system for commercial power systems with sensitive electronic loads," *IEEE Transactions on Power Delivery*, vol. 22, no. 3, pp. 1620–1627, July 2007.

[43] K. Dvijotham, E. Mallada, and J. W. Simpson-Porco, "High-voltage solution in radial power networks: Existence, properties, and equivalent algorithms," *IEEE Control Systems Letters*, vol. 1, no. 2, pp. 322–327, Oct. 2017.